

Metal-insulator transition in quasi-one-dimensional HfTe₃ in the few-chain limitScott Meyer,^{1,2,3,4,*} Thang Pham,^{1,3,4,5,*} Sehoon Oh,^{1,4} Peter Ercius,⁶ Christian Kisielowski,⁶
Marvin L. Cohen,^{1,4} and Alex Zettl^{1,3,4,†}¹*Department of Physics, University of California at Berkeley, Berkeley, California 94720, USA*²*Department of Chemistry, University of California at Berkeley, Berkeley, California 94720, USA*³*Kavli Energy NanoSciences Institute at the University of California at Berkeley, Berkeley, California 94720, USA*⁴*Materials Sciences Division, Lawrence Berkeley National Laboratory, Berkeley, California 94720, USA*⁵*Department of Materials Science and Engineering, University of California at Berkeley, Berkeley, California 94720, USA*⁶*The Molecular Foundry, One Cyclotron Road, Berkeley, California 94720, USA*

(Received 1 March 2019; revised manuscript received 7 June 2019; published 9 July 2019)

The quasi-one-dimensional linear chain compound HfTe₃ is experimentally and theoretically explored in the few- to single-chain limit. Confining the material within the hollow core of carbon nanotubes allows isolation of the chains and prevents the rapid oxidation which plagues even bulk HfTe₃. High-resolution transmission electron microscopy combined with density functional theory calculations reveals that, once the triple-chain limit is reached, the normally parallel chains spiral about each other, and simultaneously a short-wavelength trigonal antiprismatic rocking distortion occurs that opens a significant energy gap. This results in a size-driven metal-insulator transition.

DOI: [10.1103/PhysRevB.100.041403](https://doi.org/10.1103/PhysRevB.100.041403)**I. INTRODUCTION**

Constraining the physical size of solids can dramatically influence their electrical, optical, magnetic, thermal, and mechanical properties. Intrinsically low-dimensional materials, including van der Waals (vdW) bonded quasi-two-dimensional compounds [exemplified by graphite, hexagonal boron nitride, and transition-metal dichalcogenides (TMDs)] and quasi-one-dimensional vdW compounds [exemplified by transition-metal trichalcogenides (TMTs)], are particularly intriguing, in that the bulk state already presents weakened interplane or interchain bonding, which leads to strong structural, electronic, and phononic anisotropy [1,2]. Constraining the dimensions of these two-dimensional (2D) vdW materials down to “atomic thinness” can result in various degrees of additional size quantization with profound consequences. Therefore, it is a reasonable expectation that the one-dimensional (1D) vdW TMT materials would exhibit additional size quantization phenomena with novel and unexpected properties when isolated down to the few- and single-chain limit.

Recently, the prototypical quasi-one-dimensional TMT conductor NbSe₃ was successfully synthesized in the few- to single-chain limit, and unusual torsional wave instabilities were observed [3]. The driving force for the instabilities was proposed to be charging of the chains, which suggests that other TMT compounds with a closely related crystal structure might exhibit similar torsional wave instabilities in the few- or single-chain limit.

HfTe₃ is an intriguing, but little studied, group IV TMT with a trigonal prismatic linear chain structure very similar to

that of the group V TMT NbSe₃ [4–6]. Figure 1 shows the quasi-one-dimensional crystal structure of HfTe₃. Each chain distributes the Te atoms in an isosceles triangle, with the unit cell of HfTe₃ containing two trigonal prismatic chains with an inversion center. A characteristic that has inhibited extensive study of HfTe₃ is extreme air sensitivity, even for bulk single crystals [7]. Some studies [7,8] suggest that metallic HfTe₃ supports a charge density wave (CDW) and possibly filamentary superconductivity, but there are significant discrepancies between reports. Single-crystal specimens likely undergo a CDW phase transition at $T_P = 93$ K [8], while T_P for polycrystalline specimens is ~ 80 K [7,8]. Although single crystals have not shown superconductivity down to 50 mK [8], polycrystalline samples can apparently undergo a superconducting phase transition at $T_c = 1.7$ K [7].

II. METHOD

Here, we report the successful synthesis and structural characterization of HfTe₃ within the hollow cores of multiwall carbon nanotubes (MWCNTs). The selectable inner diameter of the MWCNT constrains the transverse dimension of the encapsulated HfTe₃ crystal and thus, depending on the inner diameter of the nanotube, HfTe₃ specimens with many chains (~ 20), down to few chains (three and two), and even single isolated chains, are obtained. The MWCNT sheath simultaneously confines the chains, prevents oxidation in an air environment, and facilitates characterization via high-resolution transmission electron microscopy (TEM) and scanning transmission electron microscopy (STEM). Together with complementary first-principles calculations, we find a coordinated interchain spiraling for triple- and double-chain HfTe₃ specimens, but, in sharp contrast to NbSe₃, long-wavelength intrachain torsional instabilities are markedly

*These authors contributed equally to this work.

†Corresponding author: azettl@berkeley.edu

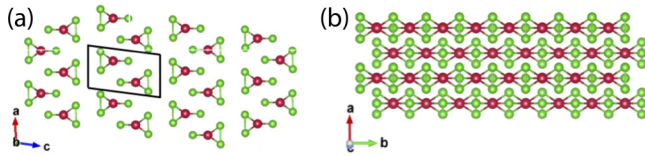


FIG. 1. Crystal view along the (a) b axis and (b) c axis, highlighting the quasi-one-dimensional nature of the trigonal prismatic HfTe_3 chains, with the unit cell boxed in black. Hf and Te atoms are represented by red and green spheres, respectively.

absent for isolated single chains. Instead, HfTe_3 shows a structural transition via a trigonal prismatic rocking distortion to a different crystal phase, concomitant with a metal-insulator transition, as the number of chains is decreased below four.

HfTe_3 is synthesized within carbon nanotubes using a procedure similar to that outlined previously for NbSe_3 [3], following HfTe_3 growth-temperature protocols [7]. Typically, stoichiometric amounts of powdered Hf along with Te shot (560 mg total), together with 1–4 mg of end-opened MWCNTs, and $\sim 5 \text{ mg/cm}^3$ (ampoule volume) of I_2 are sealed under vacuum in a quartz ampoule and heated in a uniform temperature furnace at 520°C for 7 days, then cooled to room temperature over 9 days. Energy dispersive spectroscopy (EDS) confirms a 1:3 stoichiometry of encapsulated HfTe_3 chains (25.14 at.% Hf, 74.86 at.% Te), with no statistical variations in stoichiometry along the chain observed.

III. RESULTS AND DISCUSSION

Figure 2 shows high-resolution TEM images of representative HfTe_3 samples encased within MWCNTs, together with simplified side-view and cross-sectional-view schematics. In Fig. 2(a), a 3.85-nm-wide (inner diameter) MWCNT encases ~ 20 HfTe_3 chains (the number of chains is estimated based on the carbon nanotube diameter and a close-packing configuration of the chains). Figures 2(b)–2(d) show three, two, and one HfTe_3 chain(s) within MWCNTs of inner diameters 2.50, 1.81, and 1.19 nm, respectively. We thus successfully achieve the single-chain limit of HfTe_3 . Figure 3 shows STEM images of the few- and single-chain limit of HfTe_3 samples encased within MWCNTs, with an atomic model representation of the double- and single-chain limit. Figures 3(a)–3(c) show a triple, double, and single chain of HfTe_3 confined within MWCNTs of inner diameters 2.51, 1.69, and 1.21 nm, respectively. Approximately 65% of CNT are filled, and of those filled, the total length of the chains ranges from 100 nm to over 1 μm in length.

For the related material NbSe_3 in the few-chain limit, three or two chains spiral around each other in a helical fashion, and in the single-chain limit the trigonal prismatic units comprising the chain gradually twist azimuthally as one progresses along the chain axis, comprising a single-chain torsional wave. Figures 2(b), 2(c), 3(a), and 3(b) show clearly that HfTe_3 displays the same spiraling behavior in the triple- and double-chain limit. For triple HfTe_3 chains, the spiraling node-to-node distance ranges from 3.05 to 4.44 nm [Figs. 2(b) and 3(a)], while for double HfTe_3 chains, the node-to-node distance ranges from 10.60 to 11.07 nm [Figs. 2(c) and 3(b)]. These observations demonstrate that interchain spiraling, for

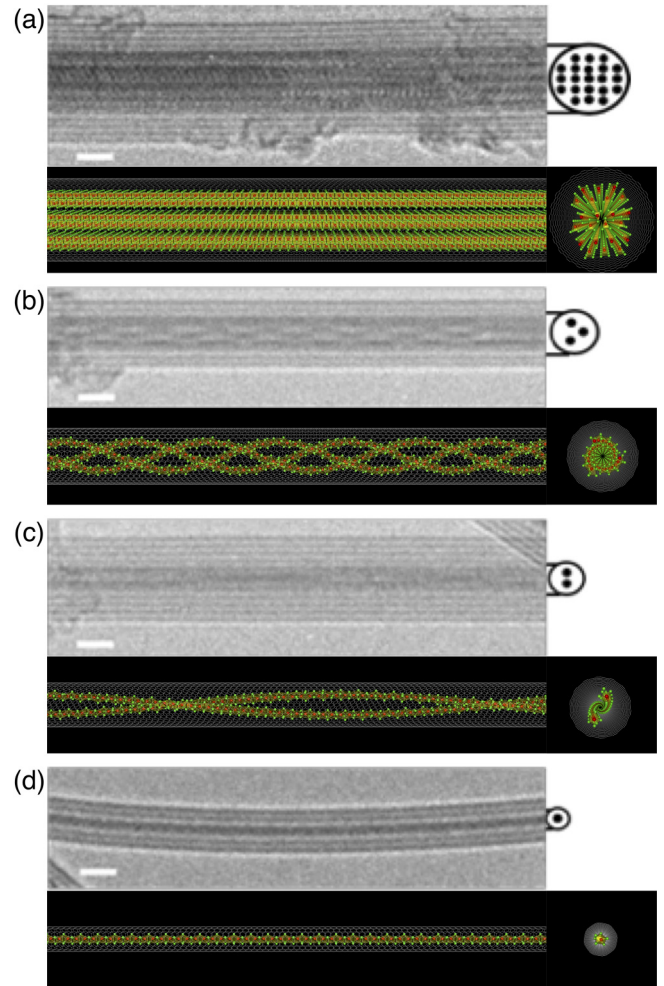


FIG. 2. Encapsulation series from many- to single-chain limit of HfTe_3 . High-resolution transmission electron microscopy images of (a) many-, (b) triple-, (c) double-, and (d) single-chain limits of HfTe_3 encapsulated within a carbon nanotube. A simplified cross-sectional representation of the filled carbon nanotube is shown to the right of each image, with a model of the chains' filling behavior shown below each image. Scale bars measure 2 nm. All images are underfocused, where Hf and Te atoms appear dark.

low chain number, is not unique to NbSe_3 —it appears to be a general feature of confined TMTs, independent of the chemical composition of the chain. The difference in node-to-node distance of the HfTe_3 chains, which is significantly longer when compared to the node-to-node distance for NbSe_3 (1.45–1.85 nm in triple-chain NbSe_3 , 1.90–2.30 nm in double-chain NbSe_3) [3], is in large part due to the larger tellurium atoms sterically preventing as tight of a spiraling overlap between the chains.

An intriguing question is, does a single chain of HfTe_3 encapsulated within a MWCNT support a torsional wave (as does a single chain of NbSe_3)? We answer our question by applying high-resolution aberration corrected high-angle annular dark field (HAADF) STEM imaging at 80 kV to encapsulated HfTe_3 . Figure 3 shows a STEM image of an encapsulated single chain of HfTe_3 , along with an atomic model, where the contrast setting does not show the CNT

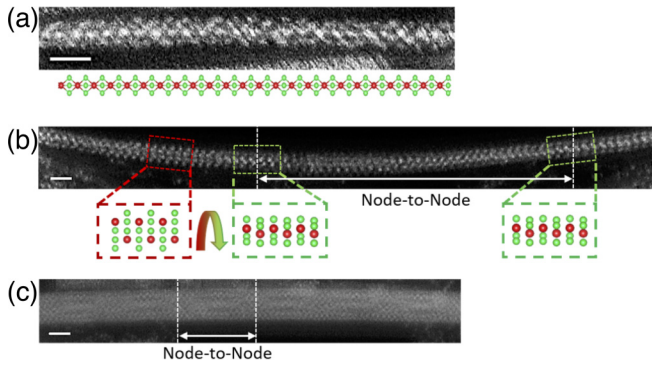


FIG. 3. Encapsulation of single, double, and triple HfTe₃ chains. Scanning transmission electron microscopy image of (a) triple, (b) double, and (c) single HfTe₃ chains encapsulated within a carbon nanotube. Hf and Te atoms appear white in the images. Atomic models below (b) and (c) demonstrate the orientation of the chain(s), where Hf and Te atoms are red and green, respectively. The node-to-node length of the spiraling in (a) and (b) is marked by white dashed lines. Scale bars measure 1 nm.

walls. Figure S1 shows additional encapsulated single-chain HfTe₃, along with a higher contrast image to show the CNT walls [9]. No long-wavelength torsional wave is observed in the single-chain limit of HfTe₃. Despite common inter-chain spiraling observed in triple and double chains of both NbSe₃ and HfTe₃, the single-chain charge-induced torsional wave (CTW) observed for NbSe₃ is absent in HfTe₃, which points to a fundamental difference between single chains of

NbSe₃ and HfTe₃. In addition, as we show below, the chains themselves in few-to-single-chain specimens of HfTe₃ display a completely different kind of structural distortion, that of intracell rocking, which, in sharp contrast to NbSe₃, results in a size-driven metal-insulator transition.

To more fully understand the structural distortions of few-to single-chain HfTe₃, we perform density functional theory (DFT) calculations. First, we investigate the atomic and electronic structures of a single chain of HfTe₃ isolated in vacuum. From the atomic positions of the chains comprising the bulk solid, we construct candidate structures using supercells with various length from $1b_0$ to $12b_0$ to investigate possible twisting behavior, where b_0 is the distance between the nearest Hf atoms. From the constructed candidate structures, atomic structures are optimized by minimizing the total energy. Unexpectedly, all investigated atomic structures of single-chain HfTe₃, except for a periodicity $\lambda = 1b_0$, show a short-wavelength rocking distortion from a trigonal prismatic (TP) unit cell [Fig. 4(c)] to a trigonal antiprismatic (TAP) unit cell [Fig. 4(h)]. This is in sharp contrast to the long-wavelength torsional wave observed in single-chain NbSe₃. Figures 4(a) and 4(b) and Figs. 4(f) and 4(g) show the atomic structure and the corresponding electronic structure of single-chain HfTe₃ in TP geometry obtained with a periodicity of $\lambda = 1b_0$, and rocked TAP geometry with $\lambda = 2b_0$. As shown in Figs. 4(i) and 4(j), the calculated electronic structure of the single-chain indicates a semiconducting transition upon isolation of a single chain, with a significant energy gap of 1.135 eV opening. Additionally, the rocked TAP structure of the HfTe₃ chains is observed in chain systems of three chains

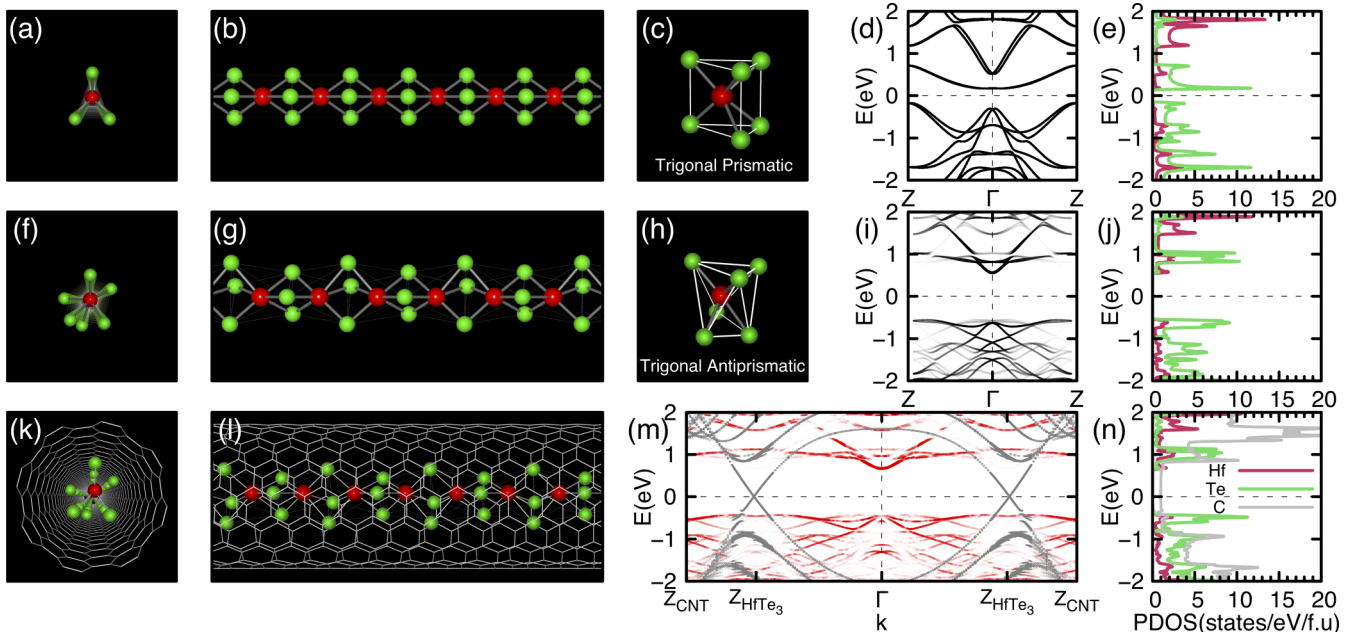


FIG. 4. Calculated atomic and electronic structures of single-chain HfTe₃. The atomic and electronic structures of single-chain HfTe₃ isolated in vacuum with (a)–(e) TP and (f)–(j) TAP geometry, and (k)–(n) the TAP single-chain encapsulated inside a (8,8) CNT are presented. In the atomic structure, the red and green spheres represent Hf and Te atoms, respectively. The basic units of (c) the TP and (h) TAP geometry are shown for comparison. In the band structures, the chemical potential is set to zero and marked with a horizontal dashed line. In (m), the bands represented by red and gray lines are projected onto the single-chain HfTe₃ and CNT, respectively, and unfolded with respect to the first Brillouin zone of the unit cell of the single chain with periodicity $\lambda = b_0$ and the CNT, where zone boundaries for the chain and CNT are denoted as Z_{HfTe_3} and Z_{CNT} , respectively.

or fewer, leading to a band-gap opening, as will be discussed in subsequent sections.

Next, we investigate the atomic and electronic structures of single-chain HfTe_3 encapsulated inside a carbon nanotube (CNT). The initial candidate structures of both TP and rocked TAP geometry single chains are constructed using the separately relaxed atomic positions of single-chain HfTe_3 isolated in vacuum, and those of an empty (8,8) CNT (indices chosen for convenience). From the candidate structures, the atomic positions of the chain are relaxed by minimizing the total energy, whereas the atomic positions of the CNT are fixed. We calculate the binding energy E_b of a single-chain HfTe_3 , which is defined as $E_b = E_{\text{HfTe}_3} + E_{\text{CNT}} - E_{\text{HfTe}_3/\text{CNT}}$, where E_{HfTe_3} is the total energy of the isolated TAP single-chain HfTe_3 , E_{CNT} is the total energy of an empty CNT isolated in vacuum, and $E_{\text{HfTe}_3/\text{CNT}}$ is the total energy of the joint system of the TP or TAP single-chain HfTe_3 encapsulated inside the CNT. The calculated binding energies of TP and TAP single chains are 0.964 and 1.23 eV per HfTe_3 formula unit (f.u.), respectively, confirming that the encapsulated single-chain HfTe_3 inside CNT also adopts a TAP geometry as in the isolated case. Because of the extremely short wavelength of the rocking TAP distortion and low signal for any diffraction studies of the chain, we are unable to resolve the TAP rocking experimentally via (S)TEM.

Figures 4(k) and 4(l) and Figs. 4(m) and 4(n) show the calculated atomic structure of single-chain HfTe_3 with TAP geometry encapsulated in the CNT and the corresponding electronic structure. The Fermi energy lies at the energy level of the Dirac point of the CNT, which is inside the gap of the single chain. As shown in Figs. 4(e) and 4(f) and Figs. 4(i) and 4(j), the states of single-chain HfTe_3 near the Fermi energy are not altered appreciably by the confinement, indicating there is no charge transfer between the HfTe_3 chain and CNT (unlike the case of encapsulated NbSe_3).

The TAP rocking in single-chain HfTe_3 versus the long-wavelength torsional wave instability observed in single-chain NbSe_3 is the most notable difference between the two systems. To explore the mechanism dictating such a drastic difference observed at the single-chain limit, two factors are key: (i) the geometry of the unit cell of the chain and (ii) the electronic structure of a single chain in each system.

Because the Te atoms in HfTe_3 are distributed as an isosceles triangle in a trigonal prismatic chain, the threefold symmetry of the chain is broken and the inversion center of the unit cell is lost when the single-chain limit of HfTe_3 is reached. This causes the Te bands near the chemical potential to split. Splitting of the bands reduces the energies of the occupied Te band near the chemical potential and creates a semiconducting gap of 0.341 eV in a single HfTe_3 chain, as shown in Figs. S3(d)–S3(f) [9]. However, the total energy of the single chain of HfTe_3 can be further lowered by rocking the Te atoms between each Hf metal center into a TAP chain, splitting the Te bands near the chemical potential even more than the TP chain, as shown in Figs. S3(g)–S3(i) [9]. The rocked TAP structure of single-chain HfTe_3 has 0.479 eV/f.u. lower total energy than the TP single chain, with the energy gap enlarging from 0.341 to 1.135 eV in the final rocked TAP structure. We note that we have also investigated an equilateral distribution of the Te atoms, similar to the Se atoms in single-

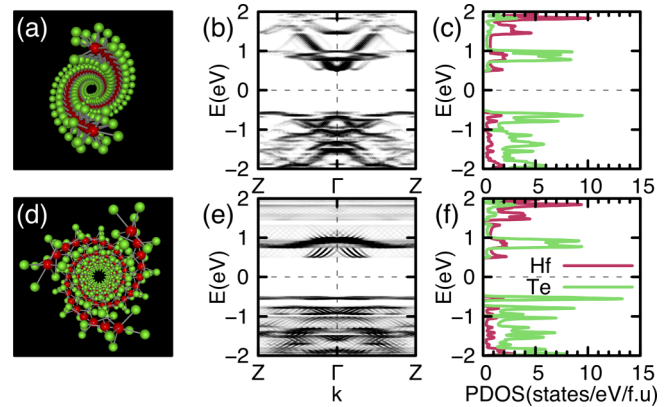


FIG. 5. Calculated atomic and electronic structures of spiraling double- and triple-chain HfTe_3 . The atomic and electronic structures of spiral (a)–(c) double and (d)–(f) triple chains of HfTe_3 isolated in vacuum are presented. In the axial view along the b axis of the unit cell, the red and green spheres represent Hf and Te atoms, respectively. In (b), (e) the band structures, the chemical potential is set to zero and marked with a horizontal dashed line and unfolded with respect to the first Brillouin zone of the unit cell of the single chain with periodicity $\lambda = b_0$, where the Brillouin zone center and the edge are denoted as Γ and Z , respectively. The individual chains comprising triple and double chains rock into TAP geometry.

chain NbSe_3 [10], shown in Figs. S3(a)–S3(c), and thereby confirmed that the isosceles distribution in HfTe_3 continues to be the energetically preferred structure for all chain numbers [9].

Splitting of the Te bands in the TAP chain is possible because the single chain of HfTe_3 has an even number of electrons in the unit cell. A single chain of NbSe_3 has an odd number of electrons in the unit cell, preventing any splitting of the bands, and allowing a metallic band structure with threefold symmetry even down to the single-chain limit. Therefore, for single-chain TMTs, we observe either a TP (NbSe_3) or TAP (HfTe_3) structural arrangement of the chalcogen atoms, depending on elemental composition, leading to metallic or insulating behavior, respectively. The structural difference between NbSe_3 and HfTe_3 is analogous to the transition-metal dichalcogenides, where some materials (such as MoS_2) prefer the trigonal prismatic ($1H$) structure showing insulating behavior, while others (such as WTe_2) prefer the trigonal antiprismatic ($1T$ or $1T'$) structure showing metallic behavior.

To investigate multichain spiraling and possible on-chain rocking of double- and triple-chain HfTe_3 , we construct several candidate structures isolated in vacuum using the atomic positions of the chains comprising the bulk solid with the diameters and periodicities of the spiral wave obtained from experimental evidence and minimize the total energy to determine the fully relaxed atomic structure. Figures 5(a)–5(c) and Figs. 5(d)–5(f) show the relaxed atomic structure, electronic band structure, and projected density of states (PDOS) of the spiraling double- and triple-chain HfTe_3 , respectively. As shown in Figs. 5(a) and 5(d), the individual chains comprising the spiral double and triple chain also rock into the TAP geometry, similar to the single-chain HfTe_3 , to minimize the

total energies of each chain. In turn, each TAP chain spirals around the others in a helical fashion. The obtained electronic structures of spiraling double-chain [Figs. 5(b) and 5(c)] and triple-chain [Figs. 5(e) and 5(f)] HfTe_3 resemble that of the TAP single chain [Figs. 4(i) and 4(j)]. Spiraling double- and triple-chain HfTe_3 has energy gaps of 1.020 and 1.018 eV, respectively, comparable to that of the TAP single chain, 1.135 eV.

To understand the preferred spiraling pattern and on-chain rocking of double- and triple-chain HfTe_3 , the competing interactions that exist among free-standing parallel chains and the interactions among encapsulated spiraling chains are analyzed. In bulk down to quadruple chains, strong interchain vdW interactions between the Hf centers and Te atoms on neighboring chains allow for the largest energy stabilization, and this is the largest determining factor in the parallel orientation of the chains. Metallic behavior is maintained from bulk to quadruple chains. Once the triple- and double-chain limit is reached, however, the chains undergo two physical changes. First, the Te ligands rock to form the TAP unit within each chain, which lowers the total chain energy and opens the energy gap. Second, the chains spiral around one another in a helical fashion. Interestingly, spiraling of the double- and triple-chain systems of HfTe_3 does not significantly alter the band gap; the rocking distortion into the TAP chain conformation remains the main driving force behind the metal-insulator transition in the few-chain limit of HfTe_3 .

IV. CONCLUSION

In summary, on-chain rocking of HfTe_3 chains into the TAP geometry drives a metal-insulator transition for chain systems of three or fewer. Quadruple- and higher-chain systems have more neighboring chains with a larger number of interchain vdW interactions between the Hf centers and

Te atoms on those neighboring chains, preventing the chains from rocking into the TAP geometry, which maintains the metallic behavior. Encapsulation of the triple- and double-chain limit within a CNT promotes the spiraling of the chains. The spiraling enhances the vdW interactions between the chains and the CNT inner wall and further stabilizes the chains.

ACKNOWLEDGMENTS

This work is primarily funded by the U.S. Department of Energy (DOE) Office of Science, Office of Basic Energy Sciences, Materials Sciences and Engineering Division, under Contract No. DE-AC02-05-CH11231 within the sp^2 -Bonded Materials Program (KC2207), which provided for synthesis of the chains, TEM structural characterization, and theoretical modeling and electronic energy band calculations of the few- and single-chain limits of HfTe_3 . The elemental mapping work was funded by the DOE Office of Science, Office of Basic Energy Sciences, Materials Sciences and Engineering Division, under Contract No. DE-AC02-05-CH11231 within the van der Waals Heterostructures Program (KCWF16). Work at the Molecular Foundry (TEAM 0.5 characterization) was supported by the DOE Office of Science, Office of Basic Energy Sciences, under Contract No. DE-AC02-05-CH11231. Support was also provided by NSF Grants No. DMR-1206512 (which provided for preparation of opened nanotubes) and No. DMR-1508412 (which provided for theoretical calculations of uncharged TMT materials).

S.M., T.P., and A.Z. conceived the idea; S.M. synthesized the materials; S.M., T.P., P.E., and C.K. conducted TEM studies; S.O. performed DFT calculations; A.Z. and M.L.C. supervised the project; and all authors contributed to the discussion of the results and writing of the manuscript.

The authors have no competing interests.

-
- [1] A. K. Geim and I. V. Grigorieva, *Nature (London)* **499**, 419 (2013).
 - [2] S. K. Srivastava and B. N. Avasthi, *J. Mater. Sci.* **27**, 3693 (1992).
 - [3] T. Pham, S. Oh, P. Stetz, S. Onishi, C. Kisielowski, M. L. Cohen, and A. Zettl, *Science* **361**, 263 (2018).
 - [4] L. Brattas and A. Kjekshus, *Acta Chem. Scand.* **25**, 2783 (1971).
 - [5] L. Brattas and A. Kjekshus, *Acta Chem. Scand.* **26**, 3441 (1972).
 - [6] J. Dai, M. Li, and X. C. Zeng, *Wiley Interdiscip. Rev. Comput. Mol. Sci.* **6**, 211 (2016).
 - [7] S. J. Denholme, A. Yukawa, K. Tsumura, M. Nagao, R. Tamura, S. Watauchi, I. Tanaka, H. Takayanagi, and N. Miyakawa, *Sci. Rep.* **7**, 45217 (2017).
 - [8] J. Li, J. Peng, S. Zhang, and G. Chen, *Phys. Rev. B* **96**, 174510 (2017).
 - [9] See Supplemental Material at <http://link.aps.org/supplemental/10.1103/PhysRevB.100.041403> for additional information on materials, characterization, and calculations, which includes Refs. [11–17].
 - [10] N. Troullier and J. L. Martins, *Phys. Rev. B* **43**, 1993 (1991).
 - [11] J. P. Perdew, K. Burke, and M. Ernzerhof, *Phys. Rev. Lett.* **77**, 3865 (1996).
 - [12] J. M. Soler, E. Artacho, J. D. Gale, A. García, J. Junquera, P. Ordejón, and D. Sánchez-Portal, *J. Phys.: Condens. Matter* **14**, 2745 (2002).
 - [13] L. Kleinman, *Phys. Rev. B* **21**, 2630 (1980).
 - [14] G. Theurich and N. A. Hill, *Phys. Rev. B* **64**, 073106 (2001).
 - [15] L. Kleinman and D. M. Bylander, *Phys. Rev. Lett.* **48**, 1425 (1982).
 - [16] S. Grimme, *J. Comput. Chem.* **27**, 1787 (2006).
 - [17] M. L. Cohen, M. Schlüter, J. R. Chelikowsky, and S. G. Louie, *Phys. Rev. B* **12**, 5575 (1975).